Journal of Hazardous Materials 192 (2011) 1675–1682

Contents lists available at ScienceDirect

Journal of Hazardous Materials

journal homepage: www.elsevier.com/locate/jhazmat

Flash fixation of heavy metals from two industrial wastes into ferrite by microwave hydrothermal co-treatment

Dan Chen [a], Chun-Yan Mei [a], Li-Hua Yao [b], Hong-Ming Jin [c], Guang-Ren Qian [a,*], Zhi-Ping Xu [d,**]

[a] College of Environmental Engineering, Shanghai University, 333 Nanchen Road, Shanghai 200444, PR China
[b] Shanghai EG Electronic Component Co., LTD., 53 Minyan Road, Shanghai 200072, PR China
[c] College of Materials Science and Engineering, Shanghai University, 149 Yanchang Road, Shanghai 200072, PR China
[d] Australian Research Council (ARC) Centre of Excellence for Functional Nanomaterials, Australian Institute for Bioengineering and Nanotechnology, The University of Queensland, Brisbane, QLD 4072, Australia

ARTICLE INFO

Article history:
Received 11 April 2011
Received in revised form 6 June 2011
Accepted 30 June 2011
Available online 23 July 2011

Keywords:
Electroplating wastewater
Pickling waste liquor
Microwave hydrothermal process
Heavy metal
Ferrite

ABSTRACT

Flash fixation of heavy metals from electroplating wastewater (EPW) and pickling waste liquor (PWL) into ferrite lattice can be investigated by microwave hydrothermal process. The toxicity of wastewater may be reduced by the redox reaction between Cr(VI) in electroplating wastewater and Fe(II) in pickling waste liquor. Box–Behnken design (BBD) experiment gives optimal process condition of ferrite formation as follows: wastewater volume ratio (V_{PWL}:V_{EPW} = 0.20), pH value 11 and retention time 15 min, on which formed ferrite has a soft magnetic property with high saturation magnetization (M_s) 47.4 emu/g. The rapid ferrite process has lower activation energy 7.01 kJ/mol according to grain growth kinetics. Concerning the environmental and economy, we introduced a new and interesting method for water remediation simultaneously synthesizing ferrite by using microwave mediated hydrothermal processes.

1. Introduction

Electroplating wastewater, a kind of industrial hazardous materials, laden with various heavy metals, such as iron (Fe), zinc (Zn), nickel (Ni) and chromium (Cr), is a potential valuable resource. Chemical precipitation, the extensively adopted method, will generate a great deal of electroplating sludge and spend high disposal cost together with secondary pollution. The electroplating sludge obtained from chemical precipitation process has been explored for making valuable ferrite with the aid of hydrothermal process. Ferrite not only is considered as important electronic material but also can be used for scavenging hazardous pollutants [1,2]. However, the ferrite product from electroplating sludge is doped with $CaCO_3$ and reflects poor saturation magnetization [3]. It is a new idea to synthesize ferrite directly from the electroplating wastewater rather than from the electroplating sludge. Additionally, direct hydrothermal process requires high temperature (300 °C) and long retention time (6 h) [3]. Comparatively, microwave hydrothermal process has some significant advantages: fast-heating and homogeneous temperature gradient [4]. Thus, in this research, our research team considers to get ferrite with high saturation magnetization from electroplating wastewater by microwave hydrothermal process.

Ferrite general formula can be expressed as XY_2O_4, where X is a divalent ion (Mg^{2+}, Fe^{2+}, Mn^{2+}, Ni^{2+}, Co^{2+}, or Zn^{2+}) or their combination, Y mainly stands for Fe^{3+} but can be substituted by any of trivalent ions (Al^{3+}, Co^{3+}, Cr^{3+}) [5]. The ideal molar ratio of trivalent to divalent ions (Y:X) is 2:1. However, the ion valence, ion varieties and their molar ratio in electroplating wastewater cannot meet this formula. For instance, it contains large amounts of toxic Cr(VI) ions with a potential risk to human, animals, and environment [6]. To satisfy Y position of trivalent ions in ferrite formula, high valence Cr(VI) must be reduced to low valence Cr(III).

In many researches, Cr(VI) has been reduced to Cr(III) by biological method [7], photo catalytic reduction [8] and reducing agent method [9]. Reducing agent was used to transfer Cr(VI) to Cr(III) by taking the advantage of elements with reducibility, e.g. Fe(II), but the reducing agents are always prepared especially. Pickling waste liquor, another industrial hazardous waste from metal surface cleaning in steel industry to improve steel surface, contains considerable amount of ferrous ions [10]. Fe(II) ions in it can serve as reducing agent to transform Cr(VI) to Cr(III). After redox reaction, trivalent and divalent metal ions can occupy Y(III) and X(II) position, respectively, but usually metal ions in solution cannot meet the molar ratio. Additional iron source has to be mixed with electroplating wastewater to adjust a suitable ratio of Y/X. As expected, Fe(II)

* Corresponding author. Tel.: +86 21 66137758; fax: +86 21 66137761.
** Corresponding author. Tel.: +61 7 33463809; fax: +61 7 33463973.
E-mail addresses: grqian@shu.edu.cn, grqian@mail.shu.edu.cn, grqian@staff.shu.edu.cn (G.-R. Qian), gordonxu@uq.edu.au (Z.-P. Xu).

0304-3894/$ – see front matter © 2011 Elsevier B.V. All rights reserved.
doi:10.1016/j.jhazmat.2011.06.091

ions in pickling waste liquor not only can achieve Cr(VI)–Cr(III) reduction transformation but also can adjust ion balance according to ferrite formula.

Therefore, the objectives of this work are (1) to reduce toxicity of wastewater through redox reaction between Cr(VI) from electroplating wastewater and Fe(II) from pickling waste liquor; (2) to realize co-treatment of these two kinds of industrial hazardous wastewaters and fix heavy metals into stable components of ferrite lattice; (3) to investigate the grain growth activation energy and demonstrate that the flash treatment by microwave hydrothermal process can be more economical than other methods.

2. Materials and methods

2.1. Materials

Electroplating wastewater A, B and C were provided by Shanghai Hazardous Waste Management Centre (Shanghai, China), the main components of which were Zn and Cr shown in Table 1. Typical pickling waste liquor, obtained from Shanghai Second Steel Co., Ltd., contained 108.5 g/L (Fe) and trace amounts of other metals, with a free acid concentration of 9.9 wt% (HCl). The chemical reagents, NaOH, HCl, acetic acid and sodium acetate were bought from Sinopharm Group Chemical Reagent Co., Ltd. with analytical grade and used as supplied.

2.2. Methods

2.2.1. Experimental procedure

To discover the co-treatment effectiveness of pickling waste liquor and electroplating wastewater, three experimental parameters, namely (i) additive volume ratio of pickling waste liquor to electroplating wastewater A (0.05–0.50) that was also referred to as wastewater volume ratio, (ii) pH value (7–11), and (iii) retention time (5–30 min), were selected as they were considered to have significant effect on the co-treatment process. For the redox reaction between Cr(VI) and Fe(II), we compared the oxidation–reduction potential (ORP) values of simulated and real mixing wastewater. At the same time, Gibbs free energy ($\Delta_r G_m$) values, residual estimate of Fe(II) and Cr(VI) in real mixing wastewater were theoretically calculated. Box–Behnken experimental design and response surface method (RSM) were used to investigate the effects of the three experimental parameters on the response functions and to determine the optimal conditions minimizing Zn and Cr leaching and maximizing saturation magnetization. Under the optimal condition, the grain growth and activation energy were described as a function of temperature and retention time.

2.2.2. Material synthesis by microwave hydrothermal method

Pickling waste liquor and electroplating wastewater were mixed together and pH values were adjusted with NaOH (5 M) controlled by pH meter (Shanghai Leici Instrument, China) to obtain precursors. Then obtained precursors were put into teflon liner reactors, transferred to the microwave oven (WP750, Guangdong Galanz Group, China) or microwave digestion system (WX-4000, Shanghai Yi-Yao Instruments, China) with rated power 750 W and heated. Products were filtered to separate solid from liquid after cooled naturally. Precipitate was washed by distilled water for 4 or 5 times following desiccation at 105 °C overnight and finally powdered.

2.2.3. TCLP

Toxicity characteristic leaching procedure (TCLP) was used to determine the chemical stability of the synthesized materials [11]. Solutions with pH of 2.88 ± 0.05 (leaching reagent A) and 4.93 ± 0.05 (leaching reagent B) were chosen as the leaching reagents. Ratio of solid to liquid was 1:20. Samples were rotated at the rate of 30 ± 2 rpm for 18 h, and filtrated after undisturbed placement for half an hour. Filtrate was kept in the plastic bottle for the toxicity analysis of heavy metal.

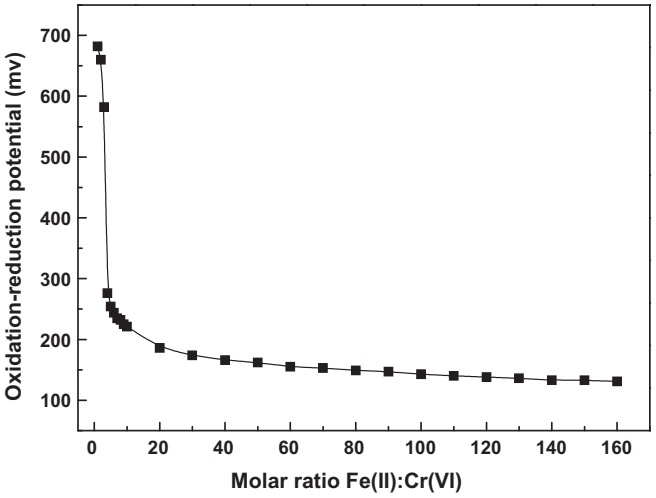

Fig. 1. Oxidation–reduction potential of simulated mixing wastewater as a function of molar ratio Fe(II)/Cr(VI).

2.2.4. Analysis

The liquid was chemically analyzed by inductively coupled plasma atom emission spectrometer (ICP-AES, Leeman Co., America). Synthesized materials were characterized by X-ray diffraction with CuKα radiation (XRD, D/MAX-2200X, Japan). Vibrating sample magnetometer (VSM, 7407 type, LakeShore Company, America) was used to measure the magnetic properties of synthesized materials. ORP values of simulated and real mixing wastewater were measured by Ag/AgCl electrode (PHS-3C pH meter, Shanghai Weiye Instrument, China).

3. Results and discussion

3.1. Redox between Cr(VI) in electroplating wastewater and Fe(II) in pickling waste liquor

In order to prove the relations of redox reaction between Cr(VI) and Fe(II), simulated mixing wastewater samples were designed with different molar ratios of Fe(II)/Cr(VI) ranging from 1 to 160 and their ORP values after the interaction were measured (Fig. 1). The ORP values for real mixing wastewater samples with wastewater volume ratio of pickling waste liquor to electroplating wastewater A rising from 0.05 to 0.50 were also measured (Table S1).

As shown in Fig. 1, ORP value for simulated mixing wastewater decreases quickly from 682 mV to 276 mV as molar ratio of Fe(II)/Cr(VI) rose from 1 to 4 initially. This result can be consistent with the reduction of Cr(VI) and the decrease in the oxidation of mixed solution. However the ORP values remain low and even invariant (less than 186 mV) as the molar ratio value of Fe(II)/Cr(VI) exceeds 20. Excessive Fe(II) ions in solution show the reduction of Cr(VI)-containing solution. The transformation of ORP from the oxidative to the reductive appears within the molar ratio value of Fe(II)/Cr(VI) rising from 4 to 20. Comparatively, ORP value for real mixing wastewater goes down from 407 mV to 194 mV as wastewater volume ratio ranges from 0.05 to 0.50 listed in Table S1. The transformation from the oxidative to the reductive can also be observed with increasing proportion of pickling waste liquor.

Table 1
Components of main metals in electroplating wastewater and pickling waste liquor.

	Elements (g/L)							
	Fe	Cu	Ni	Zn	Cr	Cd	Pb	Ca
Electroplating wastewater A	0.02	UD[a]	UD	0.28	1.61	UD	UD	0.03
Electroplating wastewater B	0.02	UD	UD	0.97	0.89	UD	UD	0.03
Electroplating wastewater C	0.02	0.01	0.01	1.63	0.30	UD	UD	0.03
Pickling waste liquor	108.47[b]	0.01	UD	0.02	0.05	0.04	0.01	UD

[a] UD related to undetected.
[b] Fe(III) is 8.96 g/L and Fe(II) is 99.51 g/L.

The reaction equation of redox between Cr(VI) in electroplating wastewater and Fe(II) in pickling waste liquor is expressed as follows:

$$Cr_2O_7^{2-} + 6Fe^{2+} + 14H^+ \rightarrow 2Cr^{3+} + 6Fe^{3+} + 7H_2O \quad (1)$$

Eq. (1) reveals that the reduction of 1 mol Cr(VI) consumes 3 mol of Fe(II). According to this, Gibbs free energy values ($\Delta_r G_m$), residual estimate of Fe(II) and Cr(VI) in real mixing wastewater can be theoretically calculated by concentrations of wastewaters and their volume ratio (Table S1). Calculated value of Gibbs free energy ($\Delta_r G_m$) increases from −233.88 kJ/mol to −223.46 kJ/mol as wastewater volume ratio rises from 0.05 to 0.50. The calculated $\Delta_r G_m$ values less than zero also demonstrate the occurrence of reaction theoretically. However, according to residual estimate of Fe(II) and Cr(VI), the redox reaction does not fully occur at wastewater volume ratio 0.05 where there are about 4.3% of Cr(VI) ions still remaining (Table S1). As wastewater volume ratio enhances from 0.07 to 0.50, residual Fe(II) ions rise from 22.5% to 89.9% (Table S1), where all the Cr(VI) ions are reduced into Cr(III). All these estimate results agree with the ORP value from high to low. Cr(III) reduced from Cr(VI) will take part in the ferrite process as cations rather than anions, which help to diminish the toxicity of wastewater and generate ferrite simultaneously.

3.2. Ferrite process during the co-treatment of electroplating wastewater and pickling waste liquor

To confirm the metastasis of metal ions from pickling waste liquor and electroplating wastewater A into precipitation phase and the occurrence of ferrite process, the concentrations of metals in treated supernatant were measured (Table 2) and precipitated phase was analyzed by XRD (Fig. 2). Single factor variables of wastewater volume ratio (0.05–0.50), pH value (7–11) and retention time (5–30 min) were discussed.

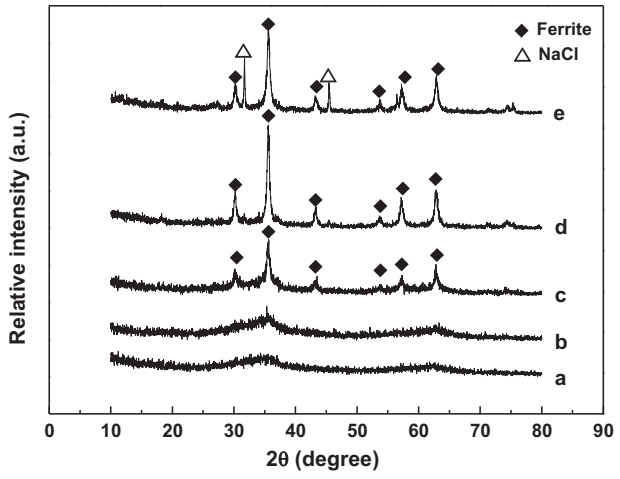

Fig. 2. XRD patterns of samples with different wastewater volume ratios (V_{PWL}:V_{EPW}): (a) 0.05, (b) 0.07, (c) 0.10, (d) 0.20, (e) 0.50.

Concentrations of metals in treated supernatant are presented in Table 2. It can be seen that as factors vary with wastewater volume ratio (0.05–0.50), pH value (7–11) and retention time (5–30 min), nearly all metal ions are transferred into the precipitation except Cr (40.8 mg/L at wastewater volume ratio 0.05) for insufficient reduction and Fe (429 mg/L at pH 7) for inadequate alkaline. XRD patterns of precipitations prepared from different wastewater volume ratios (0.05–0.50) are shown in Fig. 2. As can be seen, the samples prepared at wastewater volume ratio 0.05 and 0.07 (a and b in Fig. 2) represent amorphous without significant diffraction peaks. As shown in Table S1, 4.3% of Cr(VI) ions are surplus at wastewater volume ratio 0.05 and only 22.5% of Fe(II) ions are excess at wastewater volume ratio 0.07, indicating that most of ferrous ions take part in the redox reaction. Xu et al. [12] established that more ferrous ions existing in the precursor will promote ferrite formation. For the lack of ferrous ions, ferrite cannot be obtained. Additionally, increasing proportion of pickling waste liquor accelerates ferrite crystallization (Fig. 2c and d) as residual Fe(II) ions rises from 47.8% to 74.7% (Table S1). However, a second dominant NaCl is crystallized at wastewater volume ratio 0.50 (Fig. 2e) since pickling waste liquor carried with acid needs more NaOH to neutralize. Therefore the metastasis of metal ions into precipitation phase may be controlled by pH and ferrite process may be greatly affected by the wastewater volume ratio.

3.3. The Box–Behnken experimental design and optimization in response surface method

The Box–Behnken design (BBD), a practical experimental design method, is widely applied in the optimization of analytical methods, such as spectrum analytical method [13], chromatographic methods [14], capillary electrophoresis [15], electro analytical methods [16] and sorption process [17]. For this research, the effects of wastewater volume ratio (x_1), pH value (x_2) and retention time (x_3) are discussed. Each variable is consecutively coded as x_1, x_2 and x_3 at three levels: −1, 0 and 1. The experimental range and levels of independent variables considered in this study are presented in Table 3. The central values chosen for the experimental design are x_1 = 0.28, x_2 = 9 and x_3 = 17.5 min in uncoded form. Concentrations of Zn and Cr tested by TCLP and saturation magnetization (M_s) are designated as response values.

3.3.1. Statistical analysis

The statistical significance of the response model is evaluated by the *F*-test for analysis of variance (ANOVA). If prob > *F*-values are less than 0.05, model or model terms are significant. If values are greater than 0.10, they are not significant. As can be seen in Table 4, the prob > *F*-values for all responses are lower than 0.05 indicating that the models are significant. The coefficients of determination (R^2) close to 1 (0.8585 and 0.8152 for Zn in leaching reagent A and B, 0.9142 and 0.8500 for Cr in leaching reagent A and B, 0.9520 for

Table 2
Influence factors on treated supernatant and stability of products under optimal condition.

Samples	Conditions	Metals concentration (mg/L)				
		Cu	Zn	Ni	Fe	Cr
Wastewater volume ratio (V_{PWL}:V_{EPW}), pH = 10 ± 1, 7 ± 2 min						
0.05	Supernatant	UD	UD	UD	1.47	40.78
0.07	Supernatant	UD	UD	UD	1.11	0.39
0.10	Supernatant	0.34	UD	UD	1.24	1.37
0.20	Supernatant	UD	UD	UD	1.26	0.43
0.50	Supernatant	UD	UD	UD	1.06	0.45
pH, V_{PWL}:V_{EPW} = 0.10, 7 ± 2 min						
7	Supernatant	0.80	0.81	UD	428.77	1.49
8	Supernatant	UD	UD	UD	3.02	1.13
9	Supernatant	0.33	UD	UD	3.82	1.17
10	Supernatant	0.56	UD	UD	1.18	1.45
11	Supernatant	0.34	UD	UD	1.24	1.37
Retention time (min), V_{PWL}:V_{EPW} = 0.10, pH = 10 ± 1						
5	Supernatant	0.34	UD	UD	1.24	1.37
10	Supernatant	UD	UD	UD	4.62	1.33
15	Supernatant	UD	UD	UD	4.59	0.67
20	Supernatant	UD	UD	UD	4.48	0.56
30	Supernatant	UD	UD	UD	4.83	0.50
Optimal condition: wastewater volume ratio (V_{PWL}:V_{EPW} = 0.20),	TCLP results in leaching reagent A	UD	10.01	UD	UD	0.93
pH value 11, retention time 15 min	TCLP results in leaching reagent B	UD	UD	UD	UD	UD
	Supernatant	UD	UD	UD	UD	UD
EPA TCLP standard		15	–	–	–	5.0
GB5085.3-2007		100	100	5	–	15

Table 3
Experimental range and levels of chosen variables.

Variables	Factor	Levels		
	x	Low (−1)	Middle (0)	High (+1)
Wastewater volume ratio (V_{PWL}:V_{EPW})	x_1	0.05	0.28	0.50
pH value	x_2	7	9	11
Retention time (min)	x_3	5	17.5	30

saturation magnetization) also advocate a good correlation within the range of experiment.

3.3.2. Immobilization of Zn and Cr in synthesized ferrite

TCLP is always used to evaluate the environmental leaching risk of solid wastes, such as contaminated soils and sediments, heavy metals-bearing sludges, metallurgical process residues and combustion residues [18,19]. If the concentration of contaminants extracted exceeds regulatory limit, the waste is classified as a hazardous waste. The existent chemical species of heavy metals Zn and Cr in hydrothermal ferrite product may include chemical adsorption and chemical complex, metal oxide, hydroxide, carbonate and composite oxide. The proportion of Zn or Cr in the form of chemical adsorption, metal oxide, hydroxide and carbonate are unstable in the acid media and they are easily leached by TCLP test. However, if the ferrite process can combine heavy metals from electroplating wastewater into the lattice of spinel structure, fixed heavy metals belong to chemical stable species and even TCLP test cannot make them mobile [20]. Therefore, it is possible to assess whether Zn or Cr is chemically combined into the lattice of ferrite or not by TCLP test. The good stability of Zn and Cr corresponds to have a low leaching concentration by TCLP test.

Analysis of the variance (ANOVA) for terms can reveal their significance and helps to understand their impact degree. An analysis of the variance (ANOVA) for model terms in Fig. S1 demonstrates that, within the experimental range, only x_1 for Zn and Cr, x_2 for Zn are statistically significant. This suggests that wastewater volume ratio and pH value may affect on the response, but the effect of retention time can be ignored. To understand the reciprocal effect of wastewater volume ratio and pH on heavy metals stability, three-dimensional curves are plotted (Fig. 3) when retention time is set at 17.5 min, but the wastewater volume ratio and pH are varied from 0.05 to 0.50 and from 7 to 11, respectively.

Referring to Zn stability (Fig. 3a and b), the response surface of Zn stability in leaching reagent A has a similar pattern to that in leaching reagent B. For leaching value, Zn is considered to be more stable in leaching reagent B than in leaching reagent A due to the higher pH value for reagent B. As can be seen from Symbols A, C and D in

Table 4
Analysis of variance (ANOVA) for response model.

Response	Zn, Y_1	Cr, Y_2	Zn, Y_3	Cr, Y_4	Saturation magnetization, Y_5
	Leaching reagent A		Leaching reagent B		
	Quadratic model	Quadratic model	2FI model	Quadratic model	Quadratic model
F value	4.72	8.28	7.35	4.41	15.41
Prob > F	0.0265	0.0054	0.0032	0.0317	0.0008
R^2	0.8585	0.9142	0.8152	0.8500	0.9520

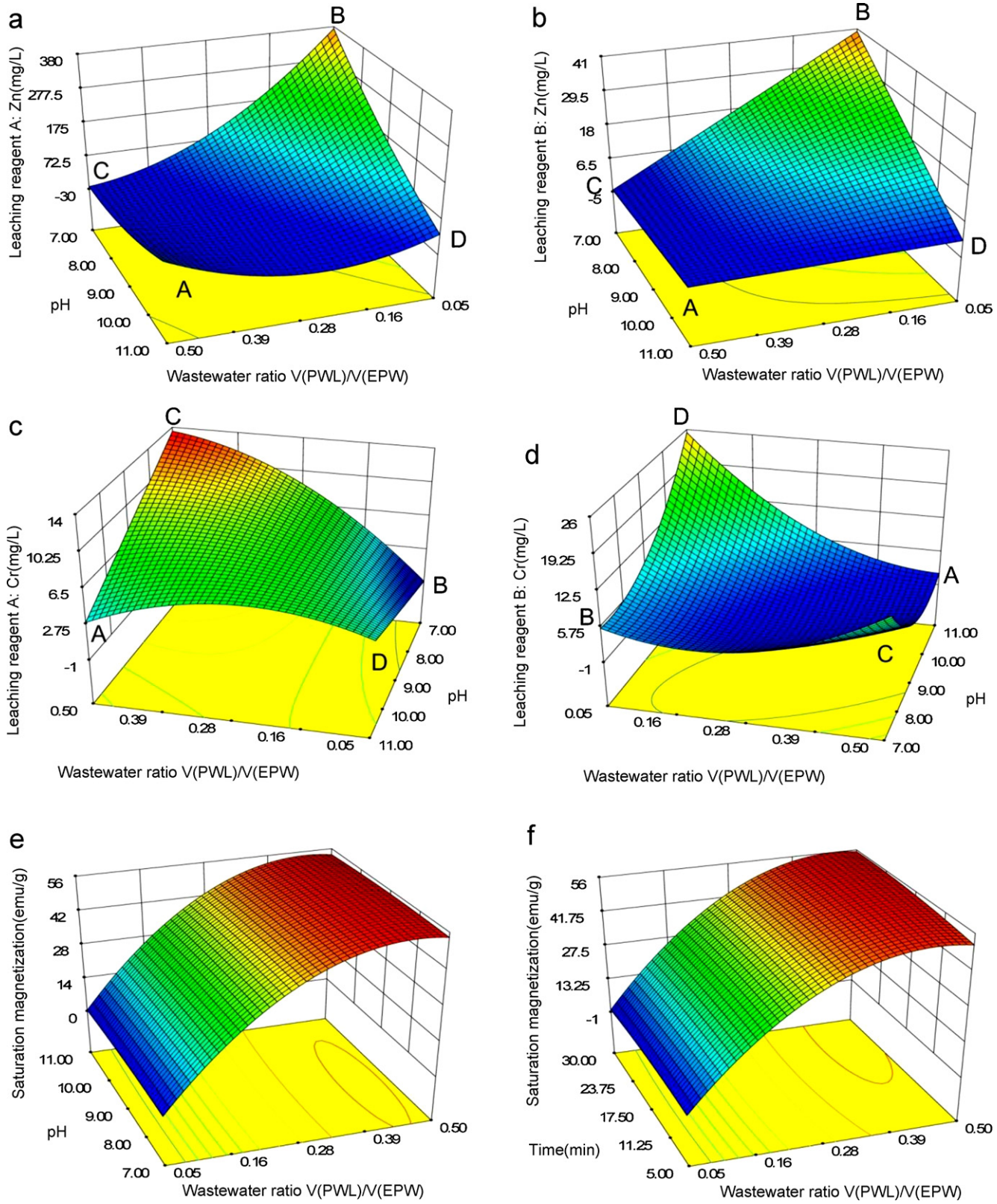

Fig. 3. Response surface curves: (a) Zn stability in leaching reagent A, (b) Zn stability in leaching reagent B, (c) Cr stability in leaching reagent A, (d) Cr stability in leaching reagent B, (e) saturation magnetization versus pH and wastewater volume ratio, (f) saturation magnetization versus retention time and wastewater volume ratio.

Fig. 3a and b, most part of Zn has a lower leaching at high wastewater volume ratio or high pH value, where leaching concentration of Zn is about 32–78 mg/L in leaching reagent A and less than 1 mg/L in leaching reagent B. This may be attributed to the ion combination of Zn(II) with Fe(III) to form zinc ferrite under alkali media. Fe(III) ions are provided by oxidization of Fe(II) from pickling waste liquor after redox reaction. However, under the circumstance of low pH value and low wastewater volume ratio (Symbol B in Fig. 3a and

b), Zn stability is decreased. The leaching concentration increases to about 380 mg/L in leaching reagent A and 40 mg/L in leaching reagent B, which is much higher than the case for high wastewater volume ratio or high pH value. The reason for this may be the obstructed metastasis of metal ions at low pH and the weakened degree of ferrite process at low wastewater volume ratio.

In terms of Cr stability (Fig. 3c and d), the situation is different. As been discussed before, a large amount of Cr(VI) ions still existed in treated supernatant due to insufficient reduction in the case of low wastewater volume ratio. As pH increases, only a small part of Cr ions can go into precipitation phase. However the poor ferrite process as described in Fig. 2a makes them leached out easily (Symbols B–D in Fig. 3c and d), the maximum leaching concentration comes up to 25 mg/L. Cr(VI) can be entirely transferred to Cr(III) with high wastewater volume ratio, but the stability of Cr still reduces as pH value decreases and the leaching concentration of Cr increases from about 1 mg/L to 13 mg/L (Symbols A–C in Fig. 3c and d). Although enough Fe(II) source transfers Cr(VI) to Cr(III), it may still induce ion competition between Cr and Fe under low pH condition where it obtains inadequate hydroxyl complexes.

3.3.3. Saturation magnetization of products

As similar analysis above, the analysis of variance (ANOVA) for saturation magnetization (Fig. S1), only x_1 is a significant model term. This indicates that only wastewater volume ratio may greatly affect on the saturation magnetization, on which parameter pH and retention time seem not to have any noticeable effect. From three-dimensional curves in Fig. 3e and f, the saturation magnetization sharply increases from about 0.5 emu/g to 35 emu/g (increases by a factor of 70) as wastewater volume ratio from about 0.05 to 0.18, under which the molar ratio of trivalent ions to divalent ones may be close to 2:1. Then saturation magnetization gradually increases from about 35 emu/g to 50 emu/g (increases by 43%) as wastewater volume ratio is between 0.18 and 0.35, on which the molar ratio of trivalent ions to divalent ones may be changed to less than 2:1 and lattice vacancy comes to be saturated. As wastewater volume ratio continues increasing, the rising trend of saturation magnetization slows down. Saturation magnetization even goes down as wastewater volume ratio exceeds 0.40. This may be caused by dosing large amounts of NaOH to neutralize acid, promoting to form NaCl crystal, and the super exchange process of ions is embarrassed [21]. Obviously, wastewater volume ratio is a controlling factor.

3.3.4. Character of ferrite formed by optimal synthesis conditions

According to significance of the response model and good correlation analyzed previously in Table 4, the responses at any regime in the interval of our experimental design can be calculated from Eqs. (2)–(6).

$$Y_1 = 13.72 - 87.51x_1 - 60.63x_2 + 8.61x_3 + 110.28x_1x_2 - 11.32x_1x_3 - 6.10x_2x_3 + 78.98{x_1}^2 + 23.06{x_2}^2 - 18.31{x_3}^2 \quad (2)$$

$$Y_2 = 9.00 - 11.41x_1 - 8.91x_2 + 4.71x_3 + 10.85x_1x_2 - 6.25x_1x_3 - 2.78x_2x_3 \quad (3)$$

$$Y_3 = 7.82 + 3.25x_1 - 1.28x_2 + 0.39x_3 - 3.98x_1x_2 + 0.085x_1x_3 + 0.58x_2x_3 - 2.77{x_1}^2 + 0.028{x_2}^2 - 0.97{x_3}^2 \quad (4)$$

$$Y_4 = -3.95x_1 + 1.82x_2 + 0.47x_3 - 8.05x_1x_2 - 0.031x_1x_3 - 0.91x_2x_3 + 5.75{x_1}^2 + 5.84{x_2}^2 - 4.93{x_3}^2 \quad (5)$$

$$Y_5 = 45.22 + 26.41x_1 - 0.44x_2 + 0.61x_3 + 0.15x_1x_2 + 1.22x_1x_3 + 4.19x_2x_3 - 17.07{x_1}^2 - 0.68{x_2}^2 - 1.13{x_3}^2 \quad (6)$$

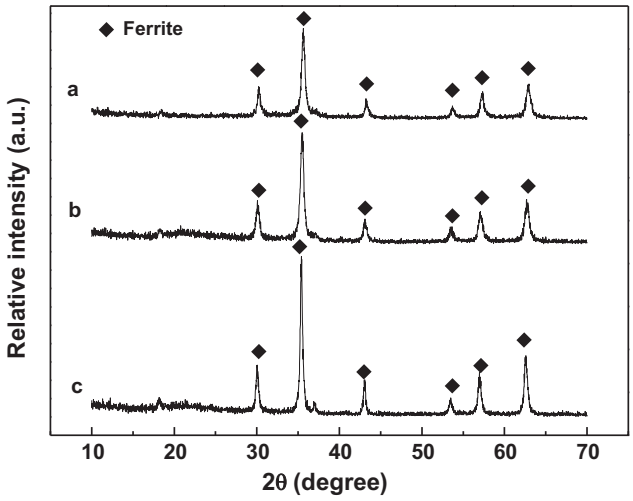

Fig. 4. XRD patterns of obtained ferrite from different electroplating wastewaters: (a) electroplating wastewater A, (b) electroplating wastewater B, (c) electroplating wastewater C.

where responses Y_1–Y_5 represent TCLP results of Zn in reagent A and B, Cr in reagent A and B and the saturation magnetization, respectively. Components x_1, x_2, x_3 represent wastewater volume ratio, pH value and retention time, respectively.

Based on these quantitative relationships, the optimal condition can be deduced, i.e. wastewater volume ratio 0.20, pH value 11 and retention time 15 min. Under this condition, electroplating wastewater A and pickling waste liquor are simultaneously treated. As displayed in Table 2, heavy metals in treated supernatant are undetected, indicating that these heavy metals are well combined into the reaction products. The XRD pattern of the precipitation (Fig. 4a) gives a typical spinel cubic structure and major product is ferrite phase without obvious second phase, showing that most heavy metals are mainly fixed into the ferrite phase. According to TCLP results summarized in Table 2, heavy metals are all undetected except 10.01 mg/L for Zn and 0.93 mg/L for Cr in leaching reagent A. This supports the fact that nearly all heavy metals are preferably stabilized in ferrite lattice. TCLP results meet the regulatory limit of TCLP in EPA and the Chinese's standard GB5085.3-2007 (Table 2). The ferrite performance tested by VSM (Fig. 5a) exhibits a

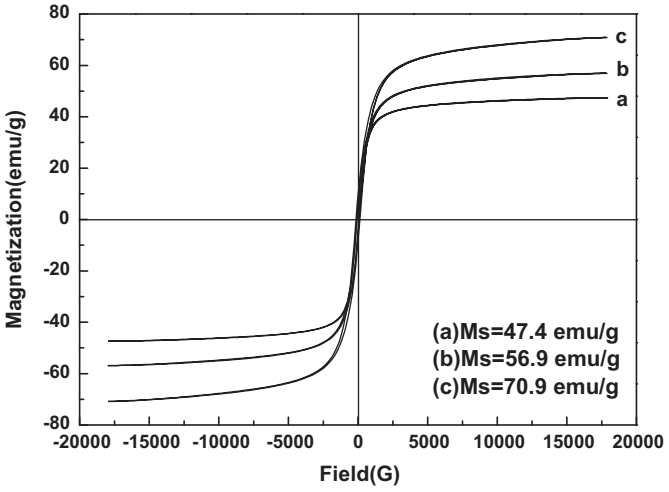

Fig. 5. Magnetization characteristic curve of ferrite from different electroplating wastewaters: (a) electroplating wastewater A, (b) electroplating wastewater B, (c) electroplating wastewater C.

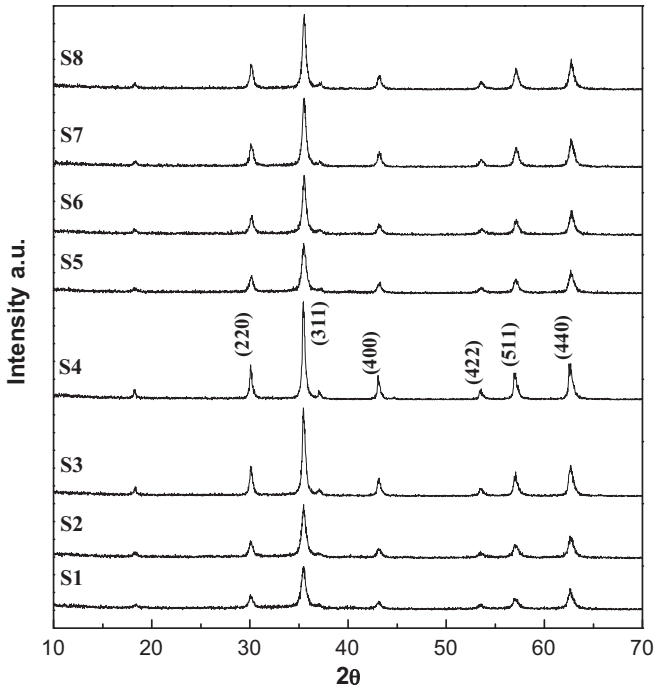

Fig. 6. XRD patterns of materials synthesized with different temperatures and times: S1: 120 °C, 50 min; S2: 150 °C, 50 min; S3: 180 °C, 50 min; S4: 210 °C, 50 min; S5: 150 °C, 10 min; S6: 150 °C, 30 min; S7: 150 °C, 70 min; S8: 150 °C, 90 min.

narrow hysteresis curve, a symbol of soft magnetic materials, with saturation magnetization (M_s) 47.4 emu/g.

3.4. Application of different electroplating wastewaters

Electroplating wastewater with different Zn and Cr concentrations (A, B and C) are used as raw materials to synthesize ferrite under optimal condition. The proportion of Cr in wastewater A, B and C is about 83%, 47% and 15%, respectively. Although major heavy metal contents of three electroplating wastewater are quite different, major products from these reaction precipitations (Fig. 6a–c) also present typical peaks of spinel cubic structure. The crystallized intensity of ferrite phase, C > B > A, hints that the presence of Cr may obstruct the crystal growth of ferrite as electroplating wastewater A contains the largest proportion of Cr. Magnetization characteristic curve of samples from electroplating wastewater A, B and C are displayed in Fig. 5a–c. The values of saturation magnetization are 47.4, 56.9 and 70.9 emu/g, respectively. Cr doping in ferrite lattice causes the poor crystallization and low magnetization. Cr(III) is known to occupy octahedral sites and reduces the density of magnetic ions in sublattice B, reducing not only the magnetic moment of the sublattice but also the exchange interaction [22]. The composition of metals in ferrite may affect the saturation magnetization.

3.5. Grain growth kinetics and activation energy

Ferrite grain size controlled by processing condition will affect the magnetic properties [23]. Generally, grain size often increases with increasing processing temperature and time [24,25] but there are exceptions for the presence of inter-granular pores [26]. Research on ferrite grain growth will help to understand the performances of the magnetic property.

The XRD patterns for the samples synthesized under optimal condition for electroplating wastewater A with temperature ranging from 120 to 210 °C and retention time from 10 to 90 min are shown in Fig. 6. The grain size for each sample is calculated using Scherrer formula (Eq. (7)) considering the most intense peak (3 1 1):

$$D = \frac{k\lambda}{\beta \cos\theta} \tag{7}$$

where D is the grain size, k is a constant equal to 0.89, λ is the X-ray wavelength equal to 0.1542 nm and β is the half-peak width.

The grain size displayed in Fig. S2a and b increases with temperature rising and retention time prolonging. The impact of temperature on grain growth is greater than that of retention time. As temperature rises from 120 °C to 210 °C, grain size grows from 20.2 to 29.5 nm, increasing by 46.0%. But the size only increases by 11.7%, from 22.3 to 24.9 nm, as retention time extends from 10 to 90 min. Raising temperature aggravates collision between ions and accelerates crystal growth rate, but prolonging retention time cannot achieve this. The reason for the flash reaction velocity of microwave hydrothermal process can be owing to its flash rising temperature.

Different grain sizes may exhibit different magnetic properties. Saturation magnetization for different grain sizes is presented in Fig. 7. It is evident from the figure that the saturation magnetization, from 41.9 to 74.8 emu/g, increases with grain size. This can be attributed to spin canting and surface spin disorder that occurred in these particles [27,28]. Smaller grain size will provide larger specific surface area. More existence of spin canting on the small grain surface may cause the decrease in saturation magnetization.

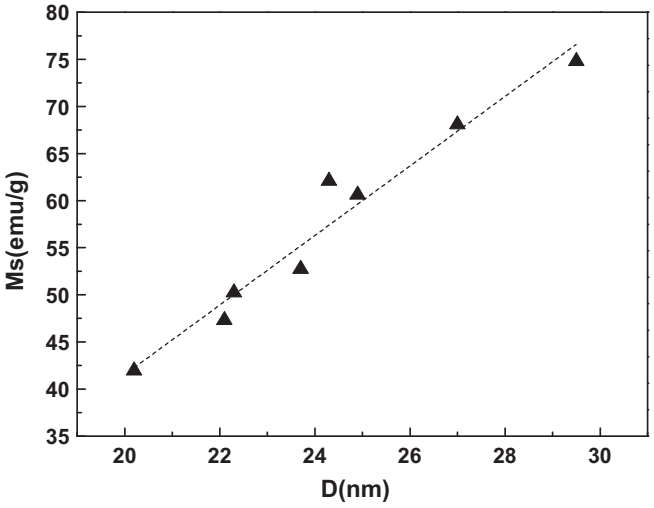

Fig. 7. Saturation magnetizations (M_s) with different grain sizes (D).

The activation energy of grain growth can be calculated by the Arrhenius equation (Eq. (8)):

$$\frac{d \ln k}{dT} = \frac{Q}{RT^2} \tag{8}$$

where k is the specific reaction rate constant, Q is the activation energy, T is the absolute temperature, and R is the ideal gas constant. The equation can be transferred to Eq. (9):

$$\log D = -\frac{Q}{2.303RT} + A \tag{9}$$

where D is the grain size and A is the intercept.

Fig. S3 shows the plots of log D versus the reciprocal of absolute temperature ($1/T$). The plot gives a good correlation with correlation coefficient R^2 0.95. The calculated activation energy is 7.01 kJ/mol. Different ferrite processes can exhibit disparate activation energy. For instance, the activation energy for high energy consuming sinter process to synthesize Mn–Zn ferrite is 71.14 kJ/mol [29]. Ni–Zn ferrite is prepared by conventional

hydrothermal process, whose activation energy is 35.06 kJ/mol [30]. Mn_3O_4 can be synthesized by solvo-thermal process with activation energy 11.36 kJ/mol [31]. Compared with those made from high energy-consuming technologies, microwave hydrothermal process has lower activation energy. It reveals that the microwave process can be carried out easily and it is more economical.

4. Conclusions

Electroplating wastewater and pickling waste liquor can be co-treated to synthesize ferrite by microwave hydrothermal process in the alkaline condition. The toxicity of wastewater can be reduced due to the redox reaction between Cr(VI) in electroplating wastewater and Fe(II) in pickling waste liquor. Under the optimal reaction condition: wastewater volume ratio (V_{PWL}:V_{EPW} = 0.20), pH 11 and retention time 15 min, pure ferrite can be obtained and it has a soft magnetic property with saturation magnetization (M_s) 47.4 emu/g. Flash rising temperature applied by microwave leads to high reaction velocity with low activation energy 7.01 kJ/mol.

Acknowledgements

This study was carried out under the key subject of Shanghai Municipality (S30109), as well as been supported by National Nature Science Foundation of China Nos. 50704023 and 50974086 and Shanghai University Excellence Youth Fund.

Appendix A. Supplementary data

Supplementary data associated with this article can be found, in the online version, at doi:10.1016/j.jhazmat.2011.06.091.

References

[1] S. Yang, Y. Guo, N. Yan, D. Wu, H. He, J. Xie, Z. Qu, J. Jia, Remarkable effect of the incorporation of titanium on the catalytic activity and SO_2 poisoning resistance of magnetic Mn–Fe spinel for elemental mercury capture, Appl. Catal. B 101 (2011) 698–708.
[2] S. Yang, Y. Guo, N. Yan, Z. Qu, J. Xie, C. Yang, J. Jia, Capture of gaseous elemental mercury from flue gas using a magnetic and sulfur poisoning resistant sorbent Mn/γ-Fe_2O_3 at lower temperatures, J. Hazard. Mater. 186 (2011) 508–515.
[3] D. Chen, J. Hou, L.H. Yao, H.M. Jin, G.R. Qian, Z.P. Xu, Ferrite materials prepared from two industrial wastes: electroplating sludge and spent pickle liquor, Sep. Purif. Technol. 75 (2010) 210–217.
[4] J.H. Lee, C.K. Kim, S. Katoh, R. Murakami, Microwave-hydrothermal versus conventional hydrothermal preparation of Ni- and Zn-ferrite powders, J. Alloys Compd. 325 (2001) 276–280.
[5] I. Mohai, J. Szépvölgyi, Treatment of particulate metallurgical wastes in thermal plasmas, Chem. Eng. Process. 44 (2005) 225–229.
[6] Z. Li, X. Zhang, L. Lei, Electricity production during the treatment of real electroplating wastewater containing Cr^{6+} using microbial fuel cell, Process Biochem. 43 (2008) 1352–1358.
[7] S.E. Lee, J.U. Lee, H.T. Chon, J.S. Lee, Reduction of Cr(VI) by indigenous bacteria in Cr-contaminated sediment under aerobic condition, J. Geochem. Explor. 96 (2008) 144–147.
[8] J. Sun, J.D. Mao, H. Gong, Y. Lan, Fe(III) photocatalytic reduction of Cr(VI) by low-molecular-weight organic acids with α-OH, J. Hazard. Mater. 168 (2009) 1569–1574.
[9] Y.M. Tzou, M.K. Wang, R.H. Loeppert, Effect of N-hydroxyethylethylenediamine-triacetic acid (HEDTA) on Cr(VI) reduction by Fe(II), Chemosphere 51 (2003) 993–1000.
[10] A. Agrawal, S. Kumari, B.C. Ray, K.K. Sahu, Extraction of acid and iron values from sulphate waste pickle liquor of a steel industry by solvent extraction route, Hydrometallurgy 88 (2007) 58–66.
[11] A.C. Sophia, K. Swaminathan, Assessment of the mechanical stability and chemical leachability of immobilized electroplating waste, Chemosphere 58 (2005) 75–82.
[12] Q. Xu, Y. Wei, Y. Liu, X. Ji, L. Yang, M. Gu, Preparation of Mg/Fe spinel ferrite nanoparticles from Mg/Fe-LDH microcrystallites under mild conditions, Solid State Sci. 11 (2009) 472–478.
[13] F.S. de Oliveira, M. Korn, Spectrophotometric determination of sulphate in automotive fuel ethanol by sequential injection analysis using dimethylsulphonazo(III) reaction, Talanta 68 (2006) 992–999.
[14] A. Stafiej, K. Pyrzynska, A. Ranz, E. Lankmayr, Screening and optimization of derivatization in heating block for the determination of aliphatic aldehydes by HPLC, J. Biochem. Biophys. Methods 69 (2006) 15–24.
[15] R. Ragonese, M. Macka, J. Hughes, P. Petocz, The use of the Box–Behnken experimental design in the optimisation and robustness testing of a capillary electrophoresis method for the analysis of ethambutol hydrochloride in a pharmaceutical formulation, J. Pharm. Biomed. Anal. 27 (2002) 995–1007.
[16] A.G. Cabanillas, M.I.R. Cáceres, M.A.M. Cañas, J.M.O. Burguillos, T.G. Díaz, Square wave adsorptive stripping voltametric determination of the mixture of nalidixic acid and its main metabolite (7-hydroxymethylnalidixic acid) by multivariate methods and artificial neural network, Talanta 72 (2007) 932–940.
[17] N. Kannan, A. Rajakumar, G. Rengasamy, Optimisation of process parameters for adsorption of metal ions on straw carbon by using response surface methodology, Environ. Technol. 25 (2004) 513–522.
[18] T. Rauckyte, D.J. Hargreaves, Z. Pawlak, Determination of heavy metals and volatile aromatic compounds in used engine oils and sludges, Fuel 85 (2006) 481–485.
[19] A. Özverdl, M. Erdem, Environmental risk assessment and stabilization/solidification of zinc extraction residue. I. Environmental risk assessment, Hydrometallurgy 100 (2010) 103–109.
[20] M. Erdem, F. Tumen, Chromium removal from aqueous solution by the ferrite process, J. Hazard. Mater. 109 (2004) 71–77.
[21] M.M. Rashad, O.A. Fouad, Synthesis and characterization of nano-sized nickel ferrites from fly ash for catalytic oxidation of CO, Mater. Chem. Phys. 94 (2005) 365–370.
[22] A. Lakshman, K.H. Rao, R.G. Mendiratta, Magnetic properties of In^{3+} and Cr^{3+} substituted Mg–Mn ferrites, J. Magn. Magn. Mater. 250 (2002) 92–97.
[23] K. Kawano, M. Hachiya, Y. Iijima, N. Sato, Y. Mizuno, The grain size effect on the magnetic properties in NiZn ferrite and the quality factor of the inductor, J. Magn. Magn. Mater. 321 (2009) 2488–2493.
[24] A.T. Raghavender, K. Zadro, D. Pajic, Z. Skoko, N. Biliskov, Effect of grain size on the Néel temperature of nanocrystalline nickel ferrite, Mater. Lett. 64 (2010) 1144–1146.
[25] K. Sun, Z. Lan, Z. Yu, X. Jiang, J. Huang, Phase formation, grain growth and magnetic properties of NiCuZn ferrites, J. Magn. Magn. Mater. 323 (2011) 927–932.
[26] M.M. Hessien, M.M. Rashad, K. El-Barawy, I.A. Ibrahim, Influence of manganese substitution and annealing temperature on the formation, microstructure and magnetic properties of Mn–Zn ferrites, J. Magn. Magn. Mater. 320 (2008) 1615–1621.
[27] Z. Gu, X. Xiang, G. Fan, F. Li, Facile synthesis and characterization of cobalt ferrite nanocrystals via a simple reduction–oxidation route, J. Phys. Chem. C 112 (2008) 18459–18466.
[28] L. Ai, J. Jiang, Influence of annealing temperature on the formation, microstructure and magnetic properties of spinel nanocrystalline cobalt ferrites, Curr. Appl. Phys. 10 (2010) 284–288.
[29] C. Liu, X. Wang, Y. Wei, Y. Jiang, Y. Yang, Study on crystallization kinetics mechanism of soft-magnetic MnZn ferrite, Rare Met. Mater. Eng. 38 (2009) 515–519.
[30] X. Li, G. Wang, Low-temperature synthesis and growth of superparamagnetic $Zn_{0.5}Ni_{0.5}Fe_2O_4$ nanosized particles, J. Magn. Magn. Mater. 321 (2009) 1276–1279.
[31] A.D. Tang, K.L. Huang, Mn_3O_4: solvo-thermal synthesis and crystallization kinetics, Chin. J. Inorg. Chem. 21 (2005) 929–932.